Discovery of selective diacylglycerol lipase β inhibitors

Zhu, N.

Chapter 5

Profiling DAGL inhibitors in the $GRAB_{eCB2.0}$ assay reveals the primary role of DAGLα in ATP-stimulated 2-AG production in Neuro2A

5.1 Introduction

The endocannabinoids 2-arachidonoylglycerol (2-AG) and anandamide (AEA) are widely distributed throughout central and peripheral nervous systems, where they play physiological roles primarily by activating cannabinoid receptors type 1 and 2 (CB_1R and CB_2R).[1] Endocannabinoids, cannabinoid receptors and enzymes responsible for the biosynthesis and degradation of endocannabinoids constitute the endocannabinoid system (ECS). In the brain, endocannabinoids are produced and released from the postsynaptic terminal upon demand[2] to activate CB_1R on the presynaptic terminal. This process is distinct from classical neurotransmitters that are stored in synaptic vesicles and released from presynaptic compartments.[3,4] In addition, glial cells[5] and intracellular organelles such as mitochondria[6,7] also contain components of the endocannabinoid system.

The biosynthesis of 2-AG is primarily mediated by *sn*1-specific diacylglycerol lipases (DAGLs), after which 2-AG is degraded by monoacylglycerol lipase (MAGL) and α/β-hydrolase domain-containing 6 and 12 (ABHD6/12) to form arachidonic acid and glycerol.[8] The production and degradation of 2-AG are tightly regulated to maintain 2-AG levels. To qualitatively and quantitatively measure 2-AG levels, liquid chromatography coupled to mass spectrometry (LC/MS) is commonly employed.[9,10] Despite being highly sensitive, this method requires sample preparation and lipid extraction, limiting its application in living cells and organisms and resulting in poor temporal and spatial resolution. In recent years, various genetically encoded fluorescent sensors[11–13] based on G protein-coupled receptors (GPCRs) and circular-permutated fluorescent proteins (cpFPs) have been developed. These sensors enable the real-time detection of neurotransmitters and neuromodulators.[14] This technology relies on the conformational change[15] of the specific receptors induced by the binding of the ligands to elicit fluorescence of cpFP. To detect the dynamics of endocannabinoids, Yulong Li's lab recently developed a GPCR activation-based endocannabinoid sensor called $GRAB_{eCB2.0}$ (Figure 5.1) based on human CB_1R and circular permutated enhanced green fluorescent protein (cpEGFP).[16] The $GRAB_{eCB2.0}$ sensor exhibits high specificity and rapid kinetics for 2-AG and AEA, and it has been successfully applied in cultured neurons, brain slices and living animals.[16–19]

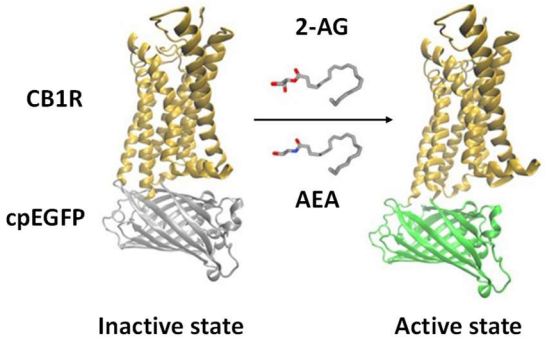

Figure 5.1 Schematic illustration of $GRAB_{eCB2.0}$ activation upon the binding of 2-AG and AEA.[16] The figure was adapted from Dong, A. *et al. Nat. Biotechnol.* **40**, 787-798 (2021).

In view of the successful applications of GRAB$_{eCB2.0}$ in monitoring the 2-AG dynamics, we aimed to develop a fluorescence-based plate reader assay by using this sensor to evaluate the cellular activity of DAGL inhibitors. To achieve this, GRAB$_{eCB2.0}$ was initially transiently transfected into mouse neuroblastoma cells (Neuro2A). The success of transient transfection and expression was confirmed by EVOS fluorescent imaging and kinetic fluorescent measurement in the plate reader. The sensor demonstrated direct activation upon the addition of 2-AG and AEA, as well as indirect activation by adding adenosine triphosphate (ATP) to the medium. Subsequently, a total of 23 DAGL inhibitors were profiled in the GRAB$_{eCB2.0}$ assay using Neuro2A cells stably expressing the sensor. This profiling revealed the primary role of DAGLα in ATP-stimulated 2-AG production.

5.2 Results and discussion

5.2.1 Transient expression and activation of the GRAB$_{eCB2.0}$ in Neuro2A

To express the GRAB$_{eCB2.0}$ sensor, Neuro2A cells were transfected with eCB2.0 plasmid. At the same time, inactive eCBmut, green fluorescent protein (GFP) and an empty vector were transfected as well to serve as controls. Strong green fluorescence was observed for Neuro2A cells transfected with GFP (Figure 5.2), indicating the success of transfection and protein expression. Green fluorescence was also detectable in cells transfected with eCB2.0, which proved that the sensor was successfully expressed in the cells and the basal level of 2-AG was able to partially activate the sensor. In contrast, the basal fluorescent signal in cells expressing inactive eCBmut was low, and no fluorescence was detected in mock transfected and untransfected Neuro2A cells. Addition of a synthetic agonist of the CB_1R, CP55,940 (1 μM), increased fluorescence in the eCB2.0 transfected but not in the eCBmut transfected cells (Figure 5.2, bottom row). The fluorescent signal was different in each Neuro2A cell because of the heterogeneity of transient expression.

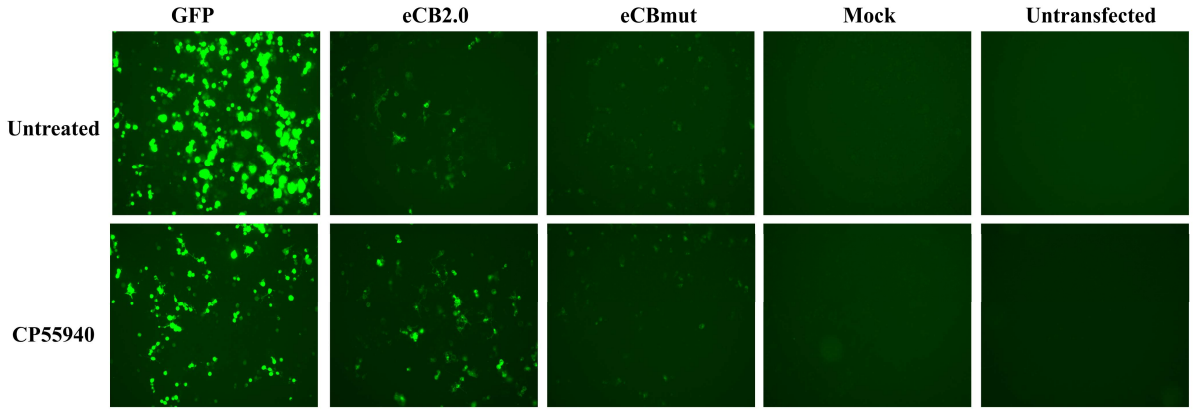

Figure 5.2 EVOS microscopy images of Neuro2A cells with different transient transfections before and after adding CB_1R agonist CP55,940.

To increase the throughput, the Neuro2A GRAB$_{eCB2.0}$ assay was adapted for a 96-well plate format. The procedure involved measuring the baseline fluorescent signal of transiently expressed GRAB$_{eCB2.0}$ in Neuro2A cells. Following this, agents were added and kinetic fluorescence measurement started immediately. Endocannabinoids 2-AG and AEA induced a concentration-dependent activation of GRAB$_{eCB2.0}$ as shown in Figure 5.3A and B. The fluorescent signal peaked within 2 min, followed by a decline and stabilization at a plateau response. 2-AG, a full agonist of CB$_1$R, increased the fluorescence by a maximum of 3-fold, which was significantly higher than the partial agonist AEA (1.5-fold). The area under the curves (AUC, Figure 5.3C, D) indicated concentration-dependent activation of GRAB$_{eCB2.0}$ in Neuro2A, with negative logarithms of half-maximal effective concentrations (pEC$_{50}$) of 6.37 ± 0.29 and 6.16 ± 0.19 for 2-AG and AEA, respectively (Figure 5.3E). Stimulation of calcium-permeable ionotropic receptors by ATP (1 mM) resulted in a pronounced increase in the fluorescence by 0.9-fold at maximum within 10 min, followed by a continuous decline (Figure 5.3F). This effect was completely blocked by CB$_1$R antagonist rimonabant (1 µM). Together, these results demonstrate that changes in GRAB$_{eCB2.0}$ fluorescence could be reliably measured in a 96-well plate reader to detect stimulus-induced 2-AG production.

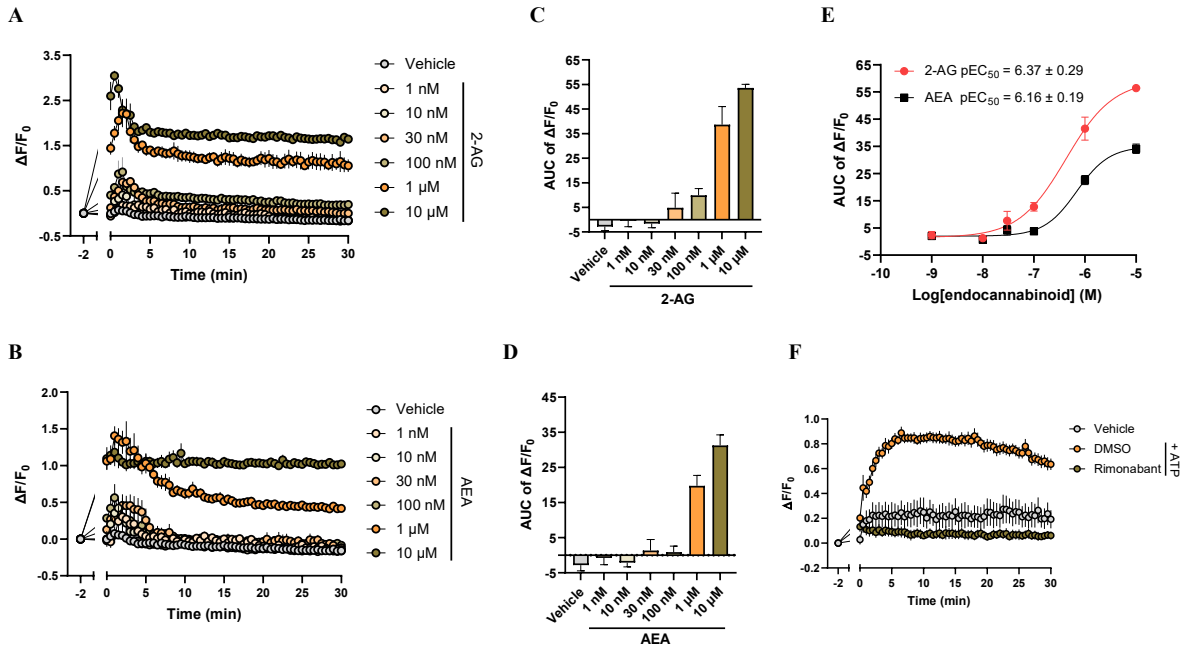

Figure 5.3 The fluorescent detection of GRAB$_{eCB2.0}$ transiently expressed in Neuro2A by a 96-well plate reader upon different stimuli. (A, B) Time course of $\Delta F/F_0$ for the vehicle and different concentrations of 2-AG (A) and AEA (B). (C, D) Area under the curve (AUC) of $\Delta F/F_0$. (E) Concentration-response curves of 2-AG and AEA. (F) Time course of $\Delta F/F_0$ for the vehicle and ATP stimulation with and without CB$_1$R antagonist rimonabant. Data shown are mean ± SEM (n = 3-6).

5.2.2 Profiling DAGL inhibitors in the Neuro2A GRAB$_{eCB2.0}$ assay

To evaluate the potential of the developed GRAB$_{eCB2.0}$ assay for assessing the cellular activity of DAGL inhibitors, Neuro2A cells stably expressing GRAB$_{eCB2.0}$ (Neuro2A GRAB$_{eCB2.0}$) were established and the inhibitory effect of DAGL inhibitors DH376 and LEI-106 on ATP-

stimulated 2-AG production was investigated. To this end, Neuro2A GRAB$_{eCB2.0}$ were seeded in a clear-bottom 96-well plate a day before the treatment. The cells were then treated with different concentrations of inhibitors or DMSO for 1 h after which the baseline fluorescence was measured. Subsequently, ATP or MilliQ (vehicle) was added and the kinetic fluorescence measurement started immediately. ATP induced a rapid and transient fluorescent signal, which was blocked by DH376 and LEI-106 in a concentration-dependent manner (Figure 5.4A, B). At the highest tested concentrations, DH376 (1 µM and 100 nM) and LEI-106 (10 µM) showed lower $\Delta F/F_0$ and AUC values than the vehicle control (Figure 5.4C, D), which might be indicative of constitutive 2-AG production. Based on AUC values, the residual activity of DAGL was calculated and plotted to obtain the concentration-response curves (Figure 5.4E, F), which showed that DH376 and LEI-106 inhibited endogenous DAGL in Neuro2A with a pEC$_{50}$ of 7.51 ± 0.20 and 5.82 ± 0.12, respectively. The activity of DH376 and LEI-106 in Neuro2A was significantly lower than their biochemical activity (Table 1), possibly due to the different affinity of these compounds to mouse and human DAGL as well as cellular permeability. Notably, the carboxyl group in LEI-106 may limit cellular permeability at physiological pH.

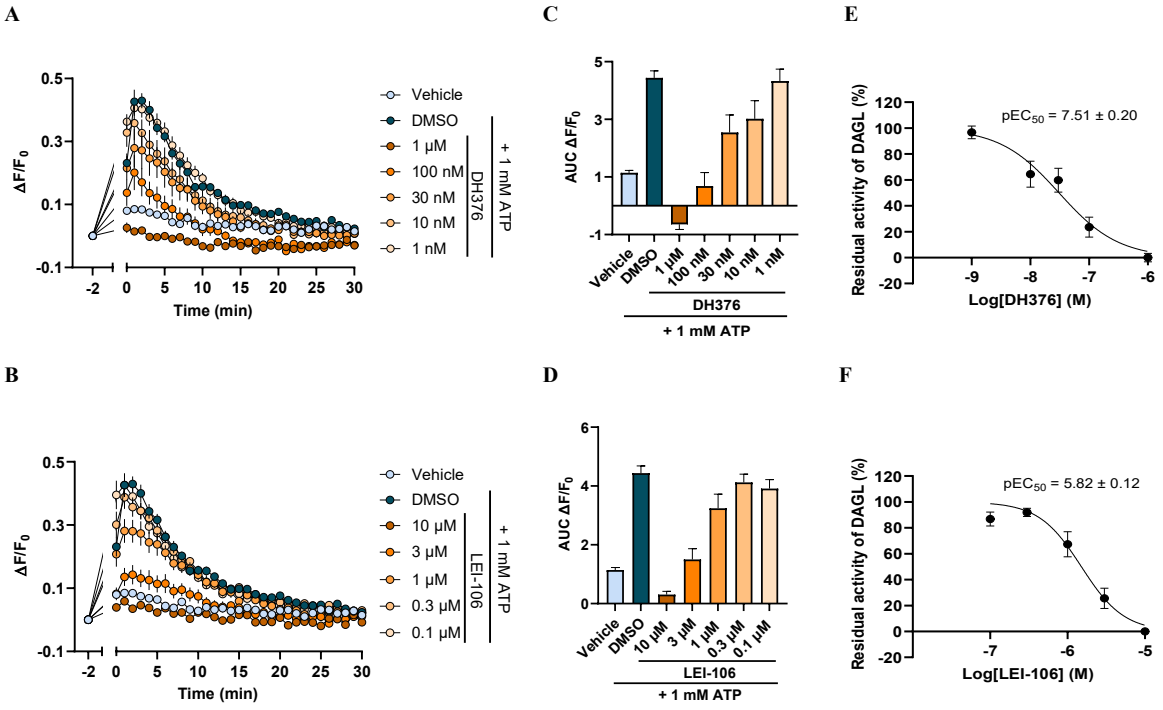

Figure 5.4 The evaluation of DAGL inhibitors DH376 and LEI-106 in the Neuro2A GRAB$_{eCB2.0}$ assay. (A, B) Time course of $\Delta F/F_0$ for the vehicle, DMSO and different concentrations of DH376 (A) and LEI-106 (B) upon ATP stimulation. (C, D) Area under the curve (AUC) of $\Delta F/F_0$. (E, F) Concentration-response curves of DH376 (E) and LEI-106 (F) with their pEC$_{50}$ values. Data shown are mean ± SEM (n = 5, N = 2).

The structure-activity relationship of glycine sulfonamides as inhibitors of DAGLα and DAGLβ was investigated in depth in Chapter 3 and 4, leading to the discovery of numerous inhibitors with varying biochemical activity and DAGL subtype selectivity. To assess their cellular inhibitory activity for DAGLs, a diverse set (chemical structures in Supplementary Figure S5.1) were tested in the Neuro2A GRAB$_{eCB2.0}$ assay within a concentration range from

10 µM to 0.1 µM. The tested inhibitors were categorized into two classes based on selectivity: non-selective DAGL and DAGLβ selective inhibitors. The concentration-response curves of non-selective DAGL inhibitors are shown in Figure 5.5 and a summary of their biochemical and cellular results is presented in Table 5.1. Similar to LEI-106, these inhibitors exhibited lower cellular activity compared to their biochemical activity. Compounds **1-5** demonstrated cellular activity with a pEC_{50} higher than 6. Among them, compound **1** displayed the highest inhibitory activity with a pEC_{50} of 6.48 ± 0.12. Compounds **6-11** were less active than LEI-106 with a pEC_{50} lower than 6. From these results, a general trend was observed that the inhibitor with a higher affinity for DAGLα would show a higher cellular activity. Notably, cellular activity can also be influenced by other factors such as lipophilicity and permeability.

The concentration-response curves of DAGLβ selective inhibitors are depicted in Figure 5.6 and their biochemical and cellular results are summarized in Table 5.2. In general, DAGLβ selective inhibitors showed lower cellular activity compared with the non-selective ones. Compounds **12-15** demonstrated activity in the Neuro2A $GRAB_{eCB2.0}$ assay with cellular activity in the micromolar range. However, the standard deviation of pEC_{50} of compounds **13-15** could not be determined due to the steep slope of the concentration-response curves. Despite being highly active for DAGLβ in the biochemical assay, compounds **16**, **17**, **19** and **20** were inactive (pEC_{50} < 5) in the Neuro2A $GRAB_{eCB2.0}$ assay. In contrast, compounds **18** and **21** showed some cellular activity.

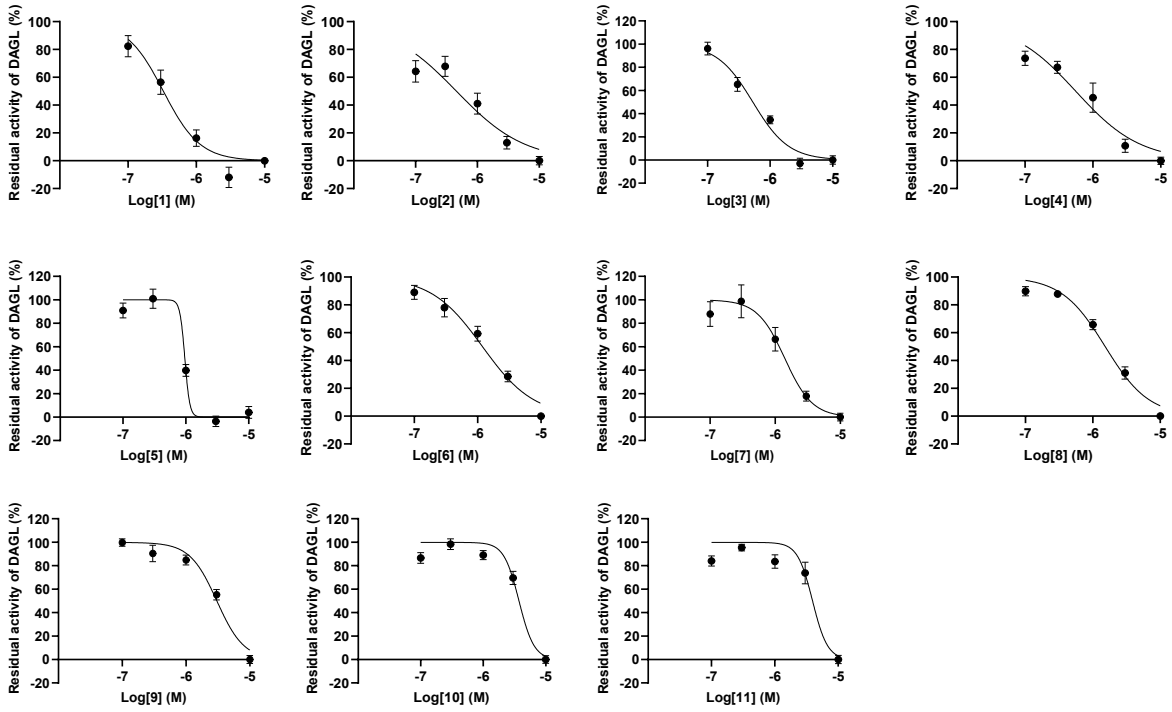

Figure 5.5 Concentration-response curves of non-selective DAGL inhibitors **1-11**. Data shown are mean ± SEM (n = 5, N = 2).

Table 5.1 Biochemical and cellular results of non-selective DAGL inhibitors **1-11**.[a]

Compound	pIC$_{50}$ DAGLβ	pIC$_{50}$ DAGLα	Apparent selectivity	cLogD	tPSA (Å^2)	pEC$_{50}$
DH376	8.79 ± 0.08	8.90 ± 0.04	0.8	4.9	80	7.51 ± 0.20
LEI-106	6.69 ± 0.14	7.35 ± 0.06	0.2	1.9	104	5.82 ± 0.12
1	7.22 ± 0.17	7.60 ± 0.08	0.4	4.5	95	6.48 ± 0.12
2	7.01 ± 0.09	7.41 ± 0.09	0.4	3.8	95	6.34 ± 0.18
3	7.22 ± 0.12	8.17 ± 0.21	0.1	3.8	95	6.28 ± 0.10
4	7.34 ± 0.18	7.89 ± 0.11	0.3	2.3	95	6.25 ± 0.15
5	7.36 ± 0.10	7.75 ± 0.11	0.4	3.2	104	6.02[b]
6	7.73 ± 0.09	7.83 ± 0.09	0.8	4.5	95	5.93 ± 0.11
7	6.96 ± 0.10	7.36 ± 0.14	0.4	4.2	95	5.85 ± 0.13
8	7.17 ± 0.10	7.20 ± 0.03	0.9	2.3	95	5.82 ± 0.07
9	7.07 ± 0.11	7.19 ± 0.04	0.8	3.0	95	5.52 ± 0.08
10	6.66 ± 0.07	6.91 ± 0.05	0.6	2.3	95	5.43 ± 0.08
11	6.66 ± 0.18	6.82 ± 0.11	0.7	4.5	95	5.40 ± 0.10

[a]The negative logarithms of half maximal inhibitory concentration (pIC$_{50}$) and half maximal effective concentration (pEC$_{50}$) were determined in DAGL EnzChek lipase substrate assay and Neuro2A GRAB$_{eCB2.0}$ assay, respectively. The calculated logarithm of the *n*-octanol-water partition coefficient at pH 7.4 (cLogD) and the topological polar surface area (tPSA) were calculated using DataWarrior 5.0.0. [b]The pEC$_{50}$ could not be reliably determined due to the steep slope of the concentration-response curves.

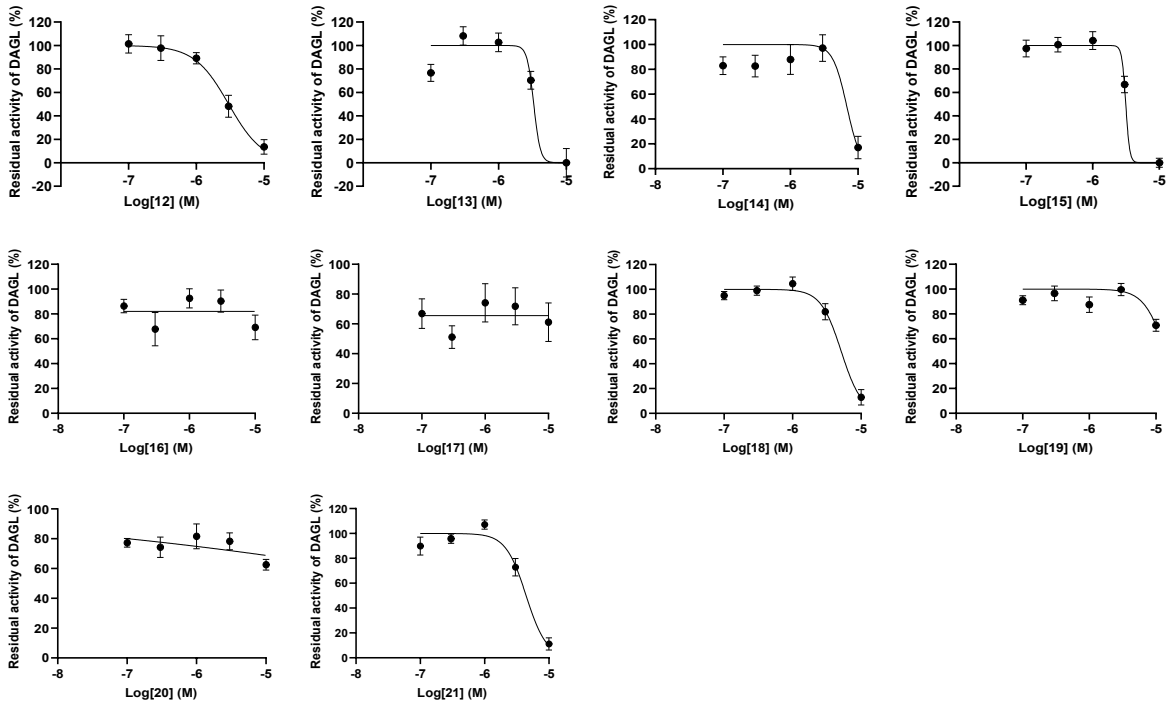

Figure 5.6 Concentration-response curves of DAGLβ selective inhibitors **12-21**. Data shown are mean ± SEM (n = 5, N = 2).

Table 5.2 Biochemical and cellular results of DAGLβ selective inhibitors **12**-**21**.[a]

Compound	pIC_{50} DAGLβ	pIC_{50} DAGLα	Apparent selectivity	cLogD	tPSA (Å²)	pEC_{50}
12	7.89 ± 0.12	7.22 ± 0.04	4.7	2.3	86	5.52 ± 0.14
13	7.85 ± 0.14	7.03 ± 0.03	6.6	2.9	99	5.48[b]
14	7.61 ± 0.12	6.50 ± 0.12	13	2.9	104	5.17[b]
15	8.29 ± 0.08	7.15 ± 0.08	14	3.2	104	5.50[b]
16	7.59 ± 0.06	6.29 ± 0.05	20	1.1	104	< 5[c]
17	7.48 ± 0.09	5.93 ± 0.16	36	1.4	104	< 5[c]
18	7.96 ± 0.06	6.37 ± 0.05	39	2.5	104	5.29 ± 0.09
19	7.94 ± 0.08	6.34 ± 0.09	40	2.2	104	< 5[c]
20	7.88 ± 0.09	6.27 ± 0.07	41	1.9	104	< 5[c]
21	8.07 ± 0.09	6.36 ± 0.05	51	2.3	104	5.35 ± 0.10

[a]The negative logarithms of half maximal inhibitory concentration (pIC_{50}) and half maximal effective concentration (pEC_{50}) were determined in DAGL EnzChek lipase substrate assay and Neuro2A $GRAB_{eCB2.0}$ assay, respectively. The calculated logarithm of the *n*-octanol-water partition coefficient at pH 7.4 (cLogD) and the topological polar surface area (tPSA) were calculated using DataWarrior 5.0.0. [b]The pEC_{50} could not be reliably determined due to the steep slope of the concentration-response curves. [c]The compound was inactive in Neuro2A $GRAB_{eCB2.0}$ assay .

5.2.3 DAGLα is responsible for ATP-stimulated 2-AG production in Neuro2A

The cellular activity of DAGL inhibitors in the Neuro2A $GRAB_{eB2.0}$ assay enabled a correlation analysis between biochemical and cellular activities to elucidate the isoform of DAGL involved in ATP-stimulated 2-AG production. For this purpose, the pEC_{50} values of the inhibitors obtained in the Neuro2A $GRAB_{eCB2.0}$ assay were plotted against the biochemical pIC_{50} values of the inhibitors for DAGLα or DAGLβ. A significant correlation between the pEC_{50} values and the pIC_{50} values for DAGLα was observed with a Pearson correlation coefficient (Pearson r) of 0.91 ($p < 0.0001$) (Figure 5.7A). Generally, inhibitors with higher affinity for DAGLα exhibited better inhibitory activity in the Neuro2A $GRAB_{eB2.0}$ assay. In contrast, there was a low correlation (Pearson r) of -0.04 ($p = 0.87$) between the pEC_{50} values and the pIC_{50} values for DAGLβ, as indicated by the scattered data points in Figure 5.7B. The non-selective and DAGLβ selective inhibitors were clustered separately, with DAGLβ selective inhibitors tending to have lower pEC_{50} than non-selective ones. Additionally, the correlation between pEC_{50} values and physiochemical properties of inhibitors, such as cLogD (representing lipophilicity) and tPSA (representing topological polar surface area), was analyzed (Figure 5.7C, D). The pEC_{50} exhibited a significant positive correlation with cLogD while displaying a negative correlation with tPSA. In this context, it cannot be ruled out that the reduced cellular activity of DAGLβ selective inhibitors in the Neuro2A $GRAB_{eCB2.0}$ assay could be attributed to generally lower lipophilicity and higher tPSA resulting in reduced cell permeability of these compounds compared to the non-selective inhibitors. Despite LEI-106 and compound **20** sharing the same tPSA and cLogD values, LEI-106 demonstrated activity in the Neuro2A $GRAB_{eCB2.0}$ assay

while compound **20** was inactive. Furthermore, compounds **14**, **15**, **18**, **19**, and **21**, possessing the same tPSA and higher cLogD compared to LEI-106, all exhibited significantly lower cellular activity than LEI-106. The reduced cellular activity in these cases was dominantly attributed to the lower potency of these compounds for DAGLα compared to LEI-106. Consequently, it can be concluded that ATP-stimulated 2-AG production in Neuro2A cells is most likely mediated by DAGLα rather than DAGLβ. Previous immunostaining studies provided valuable insights into the cellular localization of DAGLα and DAGLβ in Neuro2A cells.[20] These studies revealed that DAGLα was located on plasma membranes, whereas DAGLβ was predominantly found in perinuclear lipid droplets. The distinction in localization between DAGLα and DAGLβ may offer a plausible explanation for DAGLα's role in ATP-stimulated 2-AG production.

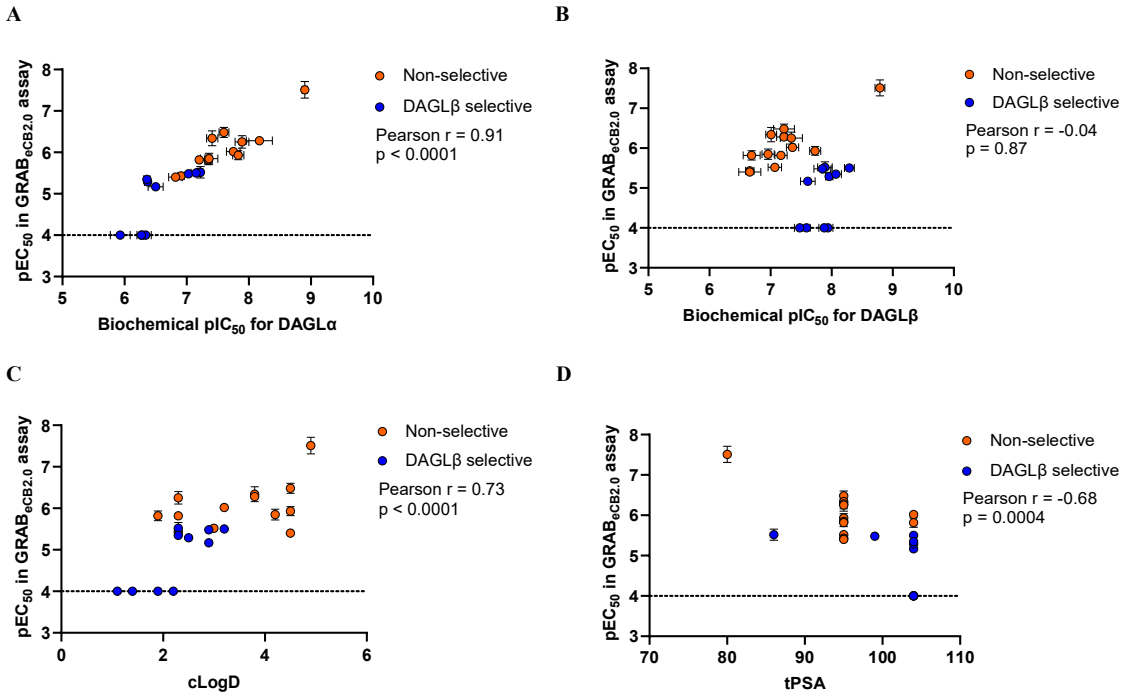

Figure 5.7 Correlation plots. (A) pEC_{50} vs biochemical pIC_{50} for DAGLα. (B) pEC_{50} vs biochemical pIC_{50} for DAGLβ. (C) pEC_{50} vs cLogD. (D) pEC_{50} vs tPSA. The pEC_{50} value for compounds that were inactive ($pEC_{50} < 5$) in the Neuro2A GRAB$_{eCB2.0}$ assay is set at 4.

5.3 Conclusion

In this Chapter, the GRAB$_{eCB2.0}$ sensor, whether transiently or stably expressed in Neuro2A cells, demonstrated exquisite sensitivity to the concentrations of 2-AG. This facilitated the kinetic measurement of ATP-induced 2-AG production in a 96-well plate format and the assessment of DAGL inhibitors in inhibiting 2-AG production. A total of 23 DAGL inhibitors with diverse activity and isoform selectivity were evaluated in the Neuro2A GRAB$_{eCB2.0}$ assay. These inhibitors concentration-dependently blocked the production of 2-AG by inhibiting DAGL with varying potencies. Correlation analysis revealed that the cellular activity of these inhibitors in the Neuro2A GRAB$_{eCB2.0}$ assay was influenced by their lipophilicity, permeability

and potency for DAGLα. Parallel comparison of the cellular activity of DAGLβ selective inhibitors and non-selective DAGL inhibitor LEI-106 with similar tPSA and cLogD values enables the conclusion that DAGLα is the dominant isoform in Neuro2A responsible for 2-AG production upon ATP stimulation. These findings further underscore the importance of isoform-specific DAGL inhibitors in unraveling the intricate mechanisms of DAGL and their roles in biological processes.

5.4 Acknowledgements

Prof. dr. Nephi Stella is gratefully acknowledged for providing plasmids of eCB2.0 and eCBmut. Tom van der Wel and Verena Straub are kindly acknowledged for generating the Neuro2A cell line stably expressing $GRAB_{eCB2.0}$. Matthijs R. van Wijngaarden is kindly acknowledged for his contribution to profiling the DAGL inhibitors in the Neuro2A $GRAB_{eCB2.0}$ assay.

5.5 Experimental methods

Cell culture

Wild type Neuro2A and Neuro2A GRAB$_{eCB2.0}$ cells were cultured at 37 °C under 7% CO_2 in Dulbecco′s modified Eagle′s medium (DMEM, Sigma Aldrich) containing phenol red, GlutaMax (2 mM), penicillin/streptomycin (200 µg/mL each, Duchefa) and 10% newborn calf serum (Thermo Fischer). Cells were passaged every 3 to 4 days and for no longer than 25 generations and the medium was refreshed every 2 to 3 days. Blasticidin S was added to the cultured Neuro2A GRAB$_{eCB2.0}$ cells once a week at a concentration of 5 µg/mL.

EVOS fluorescent microscopic imaging of Neuro2A

One day before transfection, 3×10^4 Neuro2A cells were seeded to each inner well of a clear-bottom black 96-well plate (Greiner-Bio-One, REF 655090). The outer wells were filled with 100 µL PBS (Sigma Aldrich). The cells were incubated at 37 °C under 7% CO_2 for 24 h. After that, 40 µL of medium was removed and cells were transfected with 0.3 µg PEI and 0.1 µg DNA (eCB2.0, eCBmut, GFP or empty vector) in 10 µL of serum-free DMEM. 24 h post-transfection, the medium was replaced with 100 µL PBS containing 1 mM $CaCl_2$ and 0.55 mM $MgCl_2$ and cells were incubated at rt for 20 min. Background fluorescence images were taken on Invitrogen EVOS FL Auto 2 in GFP channel. 1 µL of CB_1R agonist CP55,940 in DMSO (final concentration 1 µM) was added and fluorescence images were taken again.

2-AG, AEA and ATP Activation of GRAB$_{eCB2.0}$ in Neuro2A

Transient transfection was done as previously described. 24 h after transfection, the medium was replaced with 95 µL PBS containing 1 mM $CaCl_2$ and 0.55 mM $MgCl_2$ and cells were incubated at rt for 20 min. After incubation, baseline fluorescence was measured (30 sec/cycle, 5 cycles) in CLARIOstar® (excitation 470-15 nm, emission 515-20 nm, bottom optical, focal height ~4.1 mm). 5 µL of 2-AG or AEA at different concentrations (dissolved in PBS with 2 mg/mL BSA) was then added and kinetic fluorescence measurement (30 sec/cycle, 61 cycles) was started immediately. PBS with 2 mg/mL BSA (final concentration of 0.1 mg/mL) was used as a vehicle control. The assay was performed in n = 3. For ATP activation, 1 µL of DMSO or rimonabant at 100 µM (final concentration of 1 µM) was added followed by the baseline fluorescence measurement. 5 µL of 20 mM ATP (final concentration 1 mM) or MilliQ (vehicle) was added and kinetic fluorescence measurement started immediately. The assay was performed in n = 6. The $\Delta F/F_0$ value was calculated by the formula: $\Delta F/F_0 = (F-F_0)/F_0$, where F and F_0 represent the measured fluorescence at any time point and the baseline fluorescence, respectively. Area under the curve (AUC) of $\Delta F/F_0$ was calculated in GraphPad Prism 9.0.0, which was corrected by the AUC of vehicle to generate the concentration-response curves using GraphPad Prism 9.0.0 (nonlinear regression, log(agonist) vs. response with variable slope).

96-well plate Neuro2A GRAB$_{eCB2.0}$ assay

Neuro2A GRAB$_{eCB2.0}$ cells were harvested in fresh DMEM medium without phenol red (Sigma Aldrich) and 6×10^4 cells in 100 µL DMEM medium were seeded to each inner well of a clear-bottom black 96-well plate (Greiner-Bio-One, REF 655090). The outer wells were filled with 100 µL PBS (Sigma Aldrich). The cells were incubated at 37 °C under 7% CO_2 for 24 h. The medium was removed by aspiration and 100 µL of Hank's balanced salt solution (HBSS) with Ca^{2+} and Mg^{2+} with DMSO or inhibitor (0.1% DMSO) was added. The plate was incubated at 37 °C without CO_2 for 1 h. After incubation, baseline fluorescence was measured (60 sec/cycle, 5 cycles) in CLARIOstar® (excitation 470-15 nm, emission 515-20 nm, bottom optical, focal height ~4.1 mm, full plate gain adjustment at 25%, spiral scan, 3 mm, 25 flashes). 5.2 µL of 20 mM ATP (final concentration of 1 mM) or MilliQ (vehicle) was added and kinetic fluorescence measurement (60 sec/cycle, 31 cycles) started immediately. The $\Delta F/F_0$ value was calculated by the formula: $\Delta F/F_0 = (F-F_0)/F_0$, where F and F_0 represent the measured fluorescence at any time point and the baseline fluorescence, respectively. Area under the curve (AUC) of $\Delta F/F_0$ was calculated in GraphPad Prism 9.0.0, which was converted to the residual activity of DAGL with the formula: residual activity (%) = $(AUC - AUC_{background})/(AUC_{DMSO} - AUC_{background}) \times 100\%$, where $AUC_{background}$ represents the AUC of the vehicle control or the highest inhibitor concentration. Residual activities were used to generate the concentration-response curves using GraphPad Prism 9.0.0 (nonlinear regression, log(inhibitor) vs. normalized response with variable slope). The assay was performed in n = 5, N = 2.

References

1. Piomelli, D. The molecular logic of endocannabinoid signalling. *Nat. Rev. Neurosci.* **4**, 873–884 (2003).
2. Alger, B. E. & Kim, J. Supply and demand for endocannabinoids. *Trends Neurosci.* **34**, 304–315 (2011).
3. Südhof, T. C. Neurotransmitter release: The last millisecond in the life of a synaptic vesicle. *Neuron* **80**, 675–690 (2013).
4. Kavalali, E. T. The mechanisms and functions of spontaneous neurotransmitter release. *Nat. Rev. Neurosci.* **16**, 5–16 (2015).
5. Stella, N. Cannabinoid signaling in glial cells. *Glia* **48**, 267–277 (2004).
6. Hebert-Chatelain, E. *et al.* A cannabinoid link between mitochondria and memory. *Nature* **539**, 555–559 (2016).
7. Jimenez-Blasco, D. *et al.* Glucose metabolism links astroglial mitochondria to cannabinoid effects. *Nature* **583**, 603–608 (2020).
8. Baggelaar, M. P., Maccarrone, M. & van der Stelt, M. 2-Arachidonoylglycerol: A signaling lipid with manifold actions in the brain. *Prog. Lipid Res.* **71**, 1–17 (2018).
9. Buczynski, M. W. & Parsons, L. H. Quantification of brain endocannabinoid levels: Methods, interpretations and pitfalls. *Br. J. Pharmacol.* **160**, 423–442 (2010).
10. Marchioni, C. *et al.* Recent advances in LC-MS/MS methods to determine endocannabinoids in biological samples: Application in neurodegenerative diseases. *Anal. Chim. Acta* **1044**, 12–28 (2018).
11. Sun, F. *et al.* A Genetically Encoded Fluorescent Sensor Enables Rapid and Specific Detection of Dopamine in Flies, Fish, and Mice. *Cell* **174**, 481-496 (2018).
12. Jing, M. *et al.* A genetically encoded fluorescent acetylcholine indicator for *in vitro* and *in vivo* studies. *Nat. Biotechnol.* **36**, 726–737 (2018).
13. Wan, J. *et al.* A genetically encoded sensor for measuring serotonin dynamics. *Nat. Neurosci*. **24**, 746–752 (2021).
14. Labouesse, M. A. & Patriarchi, T. A versatile GPCR toolkit to track in vivo neuromodulation: not a one-size-fits-all sensor. *Neuropsychopharmacology* **46**, 2043–2047 (2021).
15. Vardy, E. & Roth, B. L. Conformational ensembles in GPCR activation. *Cell* **152**, 385–386 (2013).
16. Dong, A. *et al.* A fluorescent sensor for spatiotemporally resolved imaging of endocannabinoid dynamics in vivo. *Nat. Biotechnol.* **40**, 787-798 (2021).
17. Yang, N. *et al.* Deficiency in endocannabinoid synthase DAGLB contributes to Parkinson's disease and dopaminergic neuron dysfunction. *Nat. Commun.* **13**, 3490 (2021).

18. Liput, D. J. *et al.* 2-Arachidonoylglycerol mobilization following brief synaptic stimulation in the dorsal lateral striatum requires glutamatergic and cholinergic neurotransmission. *Neuropharmacology* **205**, 108916 (2022).

19. Singh, S. *et al.* Pharmacological characterization of the endocannabinoid sensor $GRAB_{eCB2.0}$. *Cannabis Cannabinoid Res.* (2023).

20. Jung, K. M., Astarita, G., Thongkham, D. & Piomelli, D. Diacylglycerol lipase-α and -β control neurite outgrowth in neuro-2a cells through distinct molecular mechanisms. *Mol. Pharmacol.* **80**, 60–67 (2011).

Supplementary Figures

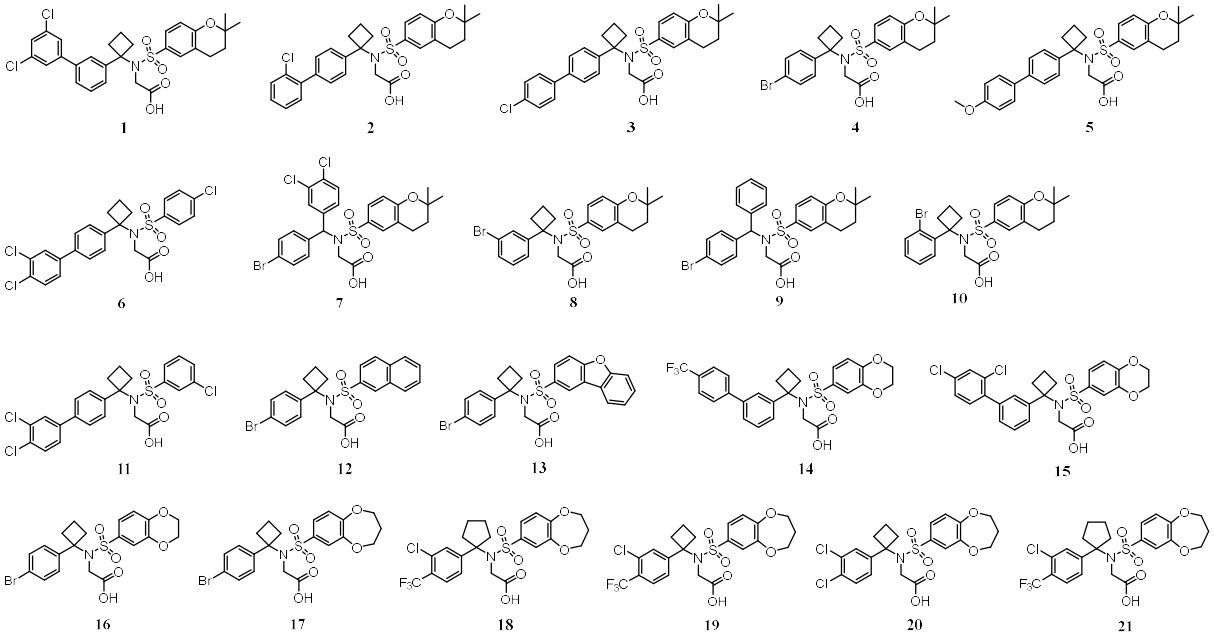

Supplementary Figure S5.1 Chemical structures of glycine sulfonamide DAGL inhibitors **1-21**.